

Secular Variation in the Interval of Outbursts in Z Cam-type Dwarf Novae

Tomohito Ohshima¹

¹*Nishi-Harima Astronomical Observatory, Center for Astronomy, University of Hyogo,
 407–2 Nishigaichi, Sayo-cho, Hyogo 679–5313, Japan
 ohshima@nhao.jp*

(Received 2022 November 8; accepted 2022 December 19)

Abstract

The secular variation in the interval of outbursts in the following six Z Cam-type dwarf novae (including the subtype IW And-type) is investigated: Z Cam, RX And, AH Her, HL CMa, SY Cnc, and WW Cet. An analysis using the $O - C$ diagram shows that the interval of outbursts is not steady in one system. The outburst properties before standstill are the decrease in outburst interval, enhancement of the magnitude in quiescence, and disappearance of the long outburst. Meanwhile, several objects have at least two typical intervals of outbursts. These characteristics are difficult to be explained only by the variation in mass transfer from the secondary.

Key words: dwarf nova — variable star

1. Introduction

Cataclysmic variables (CVs) are close binary systems consisting of a white dwarf primary and a late-type secondary filling its Roche lobe. An accretion disk is formed around the white dwarf by the material transferred from the secondary via the inner Lagrangian point (L1). Dwarf novae (DNe) are a class of CVs characterized by the presence of dwarf nova outbursts. A dwarf nova outburst is a transient event with an amplitude of several magnitudes generated on the accretion disk. The dwarf nova outburst is considered to be caused by thermal instability on the disk [for reviews, see Warner 1995; Osaki 1996; Hellier 2001].

Z Cam-type dwarf nova is a subgroup of DNe. It is characterized by an intermediate state called “standstill” in the light variations (Nijland 1930; de Roy 1932).

In general, the interval of outbursts of Z Cam-type DNe is relatively short (10–30 d). This high frequency of outbursts implies a high mass transfer rate onto the accretion disk from the secondary in Z Cam-type systems.

The accretion disk of DNe shows cycles of a high (hot) state and a low (cool) state. Meanwhile, disk instability does not occur in cases where the column density is higher than a certain borderline on the disk. In such a disk, the accretion disk is permanently hot. A dense disk is permanently hot. Therefore, such systems are called nova-like systems (NLs).

The mass transfer rate of Z Cam-type DNe is considered to lie near the borderline of the mass transfer rate \dot{M}_{crit} , i.e., the intermediate systems between DNe and NLs. Therefore, Z Cam-type systems have both phases showing a cycle of outbursts (outburst phase) and standstill. However, a certain type of variation in mass transfer rate is required to transit two states.

Meyer & Meyer-Hofmeister (1983) proposed that the irradiation effect of the secondary star by the luminosity of the ac-

cretion disk enhances the mass transfer rate. Meanwhile, Ross & Latter (2017) attempted to reproduce these without variation in mass transfer rate.

There was a debate over the cause of DN outburst, disk instability theory (DI; Osaki 1974), and enhanced mass transfer theory (EMT; Bath 1973). The variation in disk radius as outbursts repeat was revealed to correspond to the prediction by the DI theory. The debate was resolved observationally as well (Osaki & Kato 2013a; Osaki & Kato 2013b; Ohshima et al. 2014). Nevertheless, the origin of the standstill phenomenon remains unclear with respect to the DI theory.

The variation in outburst frequency is a noteworthy problem considering the role of mass transfer rate in the generation of standstill. Shafter et al. (2005) investigated the outburst interval in the Z Cam-type DN systems and demonstrated it to be moderately consistent. However, the long-term variation in outburst frequency has not been discussed fully. The variations in the interval of outbursts (t_{rec}) in Z Cam-type DNe are discussed in this paper.

2. Data set

The observation data used for this study was extracted from the AAVSO database (Kafka 2021), VSNET data (Kato et al. 2004), ASAS-SN Sky Patrol data (Shappee et al. 2014), ASAS3 System data (Pojmański 2002), and Zwicky Transient Facility data (Masci et al. 2019; Bellm et al. 2019). The span of the data used is 2450000–2459884 (approximately 27 years).

The target systems are selected from among the brightest group of Z Cam-type DN systems. The number of known Z Cam-type systems is 327. These are listed in International Variable Star Index (VSX)¹. Meanwhile, 44 are listed in the

¹ <https://www.aavso.org/vsx/>

General Catalogue of Variable Stars (GCVS). This significant difference is largely owing to the non-registration (in GCVS) of objects newly identified by deep sky-survey. These objects are significantly faint and thereby, are difficult to be monitored adequately.

The brightest six objects are selected in this study: Z Cam, RX And, WW Cet, HL CMA, AH Her, and SY Cnc. Although IX Vel is the brightest Z Cam-type object in VSX, it had not been considered as a DN object until recently (Kato 2020). The fundamental property of the six objects is summarized in Table 1.

The outburst timings are determined based on the light curve. Therefore, the start date of brightening should be used if observed. However, the gap between observations inhibits this clear estimation because the observations are generally few in the long-term monitoring light curve. Thus, the date on halfway of rising or the earliest date the main outburst is used in many cases. Thereby, errors of a few days occur in the determination of the start date of outbursts. Additionally, the conjunction with the sun makes seasonal gap of observations, which usually includes several outbursts, is inevitable.

Therefore, observed-minus-calculated ($O - C$) diagrams are adopted in this research to investigate the long-term variations in t_{rec} .

3. Result and Analysis

3.1. Z Cam

Z Cam is a prototype object of Z Cam-type systems. Oppenheimer et al. (1998) analyzed AAVSO observation data and indicated the long-term variation in t_{rec} . However, the interval in this study is based on the moving average with the 1500-day window. Thus, the variations in t_{rec} in the shorter term (i.e., in the timescale of months or a few years) cannot be detected.

The light curve is shown in Figure 1. The Z Cam light variation broadly includes two phases, or standstill phases, and outbursts occur consecutively (outburst phase). According to the light curve, the light variation is divided into 13 outburst phases and standstill phases between these. The corresponding range for each outburst phase is plotted in Figure 2 (I–XIII). Although the standstill phase is not plotted in this diagram, the journal of standstill in Z Cam is summarized in Table 2.

Linear regression is used to estimate the mean t_{rec} with the dates of the outbursts obtained. The period obtained is 27.61(6) d. The ephemeris JD of the outburst start date (JD_{os}) is calculated based on this period by using the following ephemeris equation:

$$JD_{\text{os}} = 2449928.7 + 27.61 \times E$$

The value of the $O - C$ diagram with the ephemeris calculated using this equation is presented in Figure 2.

This diagram indicates the secular variation in t_{rec} . The $O - C$ diagram is divided by the standstill. The seasonal gap is insignificant because Z Cam can be observed throughout the year in the northern hemisphere. Rather, the $O - C$ diagram has a gap owing to a standstill.

Because a large increase is observed in the $O - C$ diagram if the number of outbursts is assumed as zero, the cycle number is offset by a whole-number multiple of intervals near the length

of a standstill.

The characteristics seen outbursts before the start of standstill is widely seen;

(1) the minimum magnitude becomes brighter (typically 0.5 mag);

(2) the duration of outbursts reduces;

(3) the interval of outbursts reduces.

(1) cannot be observed in certain cases (OP VIII, XII, and XIII). This may be because of the data scattering. (2) includes the most pronounced characteristics.

(3) is not observed in OP VI and VII. However, these OPs are relatively peculiar. The outburst frequency in the earlier stage of OP VI is low because of the circumvention of small outbursts considering the difficulty of determining their start timings. Thus, the estimated t_{rec} is significantly long. This peculiar phase ends in the subsequent stage of OP VI.

OP VII is also atypical. The termination timing of the standstill between OP VI and VII is ambiguous because the standstill (when the luminosity was almost constant) smoothly transited the small oscillation. Such oscillation is generally observed at the beginning or the final stage of the standstill (Szkody & Mattei 1984). However, in this case, the amplitude of oscillations increased and showed a smooth transition to the outburst of OP VII. Thus, the outbursts in the early and middle stages of OP VII outbursts may be interpreted as oscillations. Only the final three outbursts are considered to be ordinary outbursts.

The $O - C$ diagram shows that the t_{rec} of Z Cam is inconsistent. In addition, the interval length varies abruptly (rather than gradually) during the outburst phase.

Oscillations are observed at the beginning (cf: SS IV) or the final stage (cf: SS IX) of certain cases of standstill. This is similar to the phenomenon reported in Kato (2001).

3.2. RX And

RX And is one of the most popular Z Cam-type dwarf novae. It is also known to have undergone an episode of a substantial decline in 1997 (Kato et al. 2002). It showed a similar (albeit significantly shorter decline) episode in 2000². These phenomena imply that RX And has a certain mechanism that causes the reduction in mass transfer rate to be nearly zero. Hence, this system could play an important role in this study.

The entire light curve is presented in Figure 3. The data used starts immediately after the standstill (JD 2449900–2450300) and a substantial decline (JD 2450300–2450450). Ordinary variations begin to be observed after JD 2450600. The cycle number of outbursts is counted the standstill after that.

RX And can be observed in almost all the seasons in the northern hemisphere. However, the observation condition is less favorable than that for Z Cam because RX And is closer to the zodiac than Z Cam. Thus, the seasonal gap is observed more frequently than for Z Cam. The cycle number is estimated by the extrapolation with the date and the preceding interval.

The outburst phase is divided into 14 phases. Unlike One outburst phase (OP V) is terminated by the long minimum instead a standstill.

² [vsnet-alert 4863], <http://www.kusastro.kyoto-u.ac.jp/vsnet//Mail/alert4000/msg00863.html>

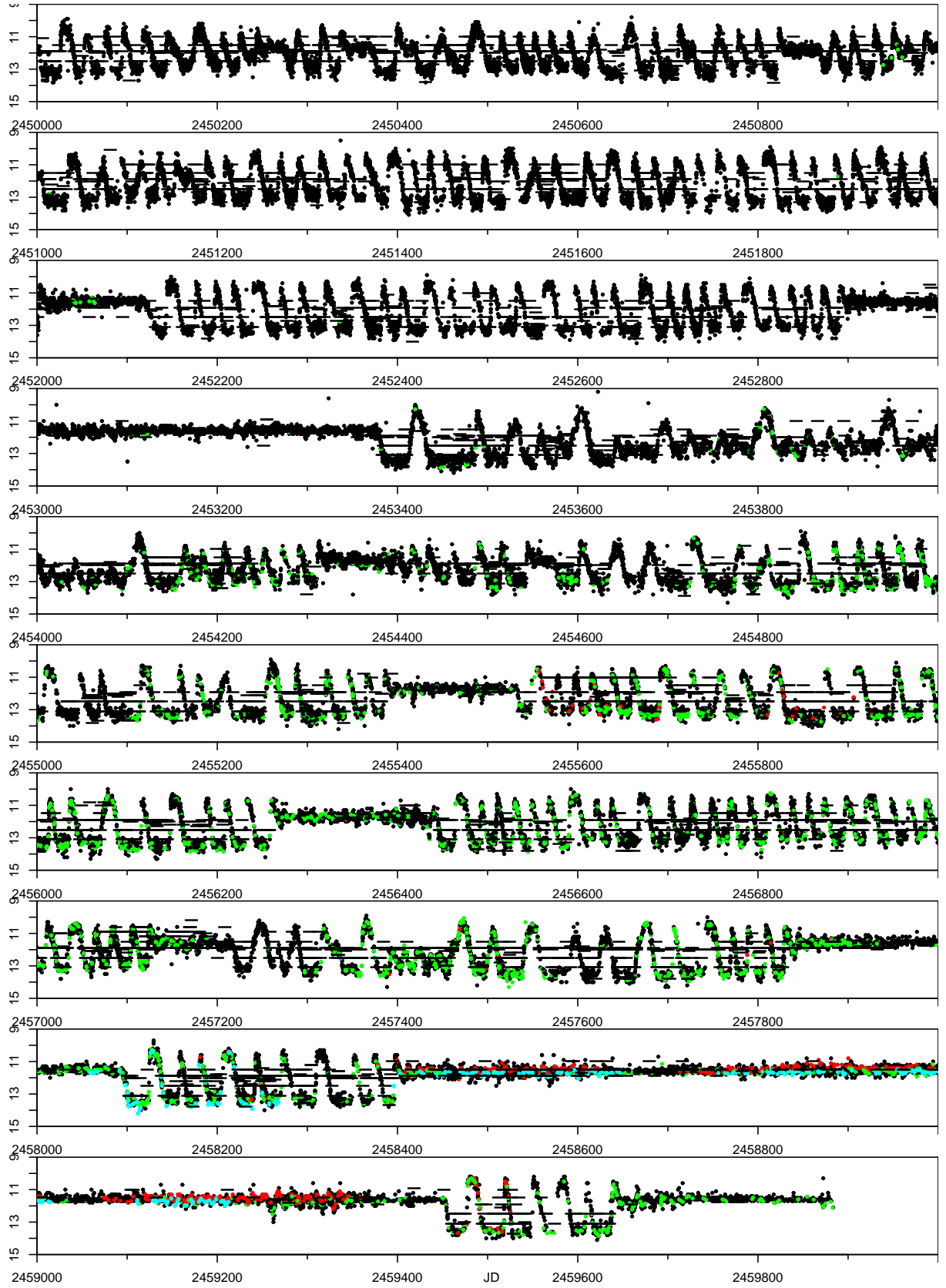
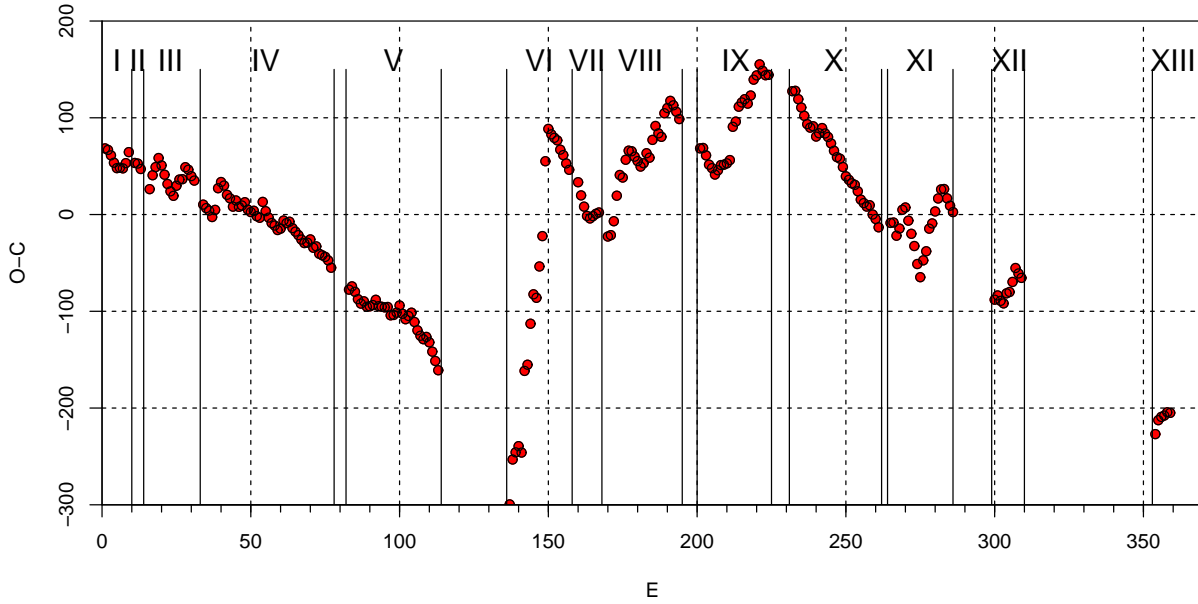


Fig. 1. Z Cam light curve of the entire span. The y-axis represents the magnitude. The color bands are as follows: the visual data (black circle), the V (green circle) or CV (blue circle) band on the CCD data, and the cG (red circle) band of digital camera photometry. The bar represents the upper limit when not observed.

Table 1. Target List

Object	M_{\max}	M_{\min}	Orbital Period (d)	Remarks
Z Cam	10.0	14.5	0.289841	
RX And	10.3	14.8	0.209893	
WW Cet	10.4	15.8	0.17578	
HL CMa	10.7	15.0	0.216787	IW And type
AH Her	10.8	14.9	0.258116	IW And type
SY Cnc	11.0	14.0	0.3823753	

The data of the range of variation in magnitude (maximum M_{\max} , minimum M_{\min}) of variations is retrieved from GCVS 5.1. The data of the orbital period is retrieved from RKCate Ritter & Kolb (2003).

**Fig. 2.** Complete $O - C$ diagram of Z Cam. The x-axis represents the number of cycles, and the y-axis represents the $O - C$ value calculated with the ephemeris equation described in this paper. The Roman numbers I–XIII represent the outburst phases (divided with solid lines).**Table 2.** Z Cam Standstill List

	Period (JD–2400000)	Duration (d)
SS I	50249–50275	26
SS II	20349–50372	23
SS III	50830–50868	38
SS IV	52012–52123	111
SS V	52899–53379	480
SS VI	54321–54380	59
SS VII	54552–54572	20
SS VIII	55393–55532	139
SS IX	56270–56443	163
SS X	57131–57217	86
SS XI	57840–78096	156
SS XII	58407–9453	1046
SS XIII	9650–	-

t_{rec} is determined to be 15.239(13) d by performing linear regression on the data. Szkody & Mattei (1984) reported the mean period of RX And as 13 d (scattering 5–20 d).

The following is the ephemeris equation:

$$JD_{\text{os}} = 2450765 + 15.239 \times E$$

The $O - C$ diagram calculated with this equation is presented in figure 4. OP VIII appears to have an irregularly long interval. However, this case is similar to OP VI of Z Cam. That is, small short outbursts are observed frequently, and their start timings are difficult to determine. The light curve and $O - C$ diagram reveal that the characteristics identified in Z Cam (1)–(3) are observed in RX And as well.

Long-continued outburst phases such as OP VI, X, and XII show a cyclic variation in the $O - C$ value. This more or less corresponds to the cyclic variation in luminosity in quiescence. However, the cyclic variation in $O - C$ occurs abruptly. Meanwhile, the variation in luminosity in quiescence occurs more gradually. Figure 4 shows two types of gradients: the downward-sloping curve and the upward-sloping curve. This implies that the $O - C$ curve is composed of two periods: 14 d and 17 d.

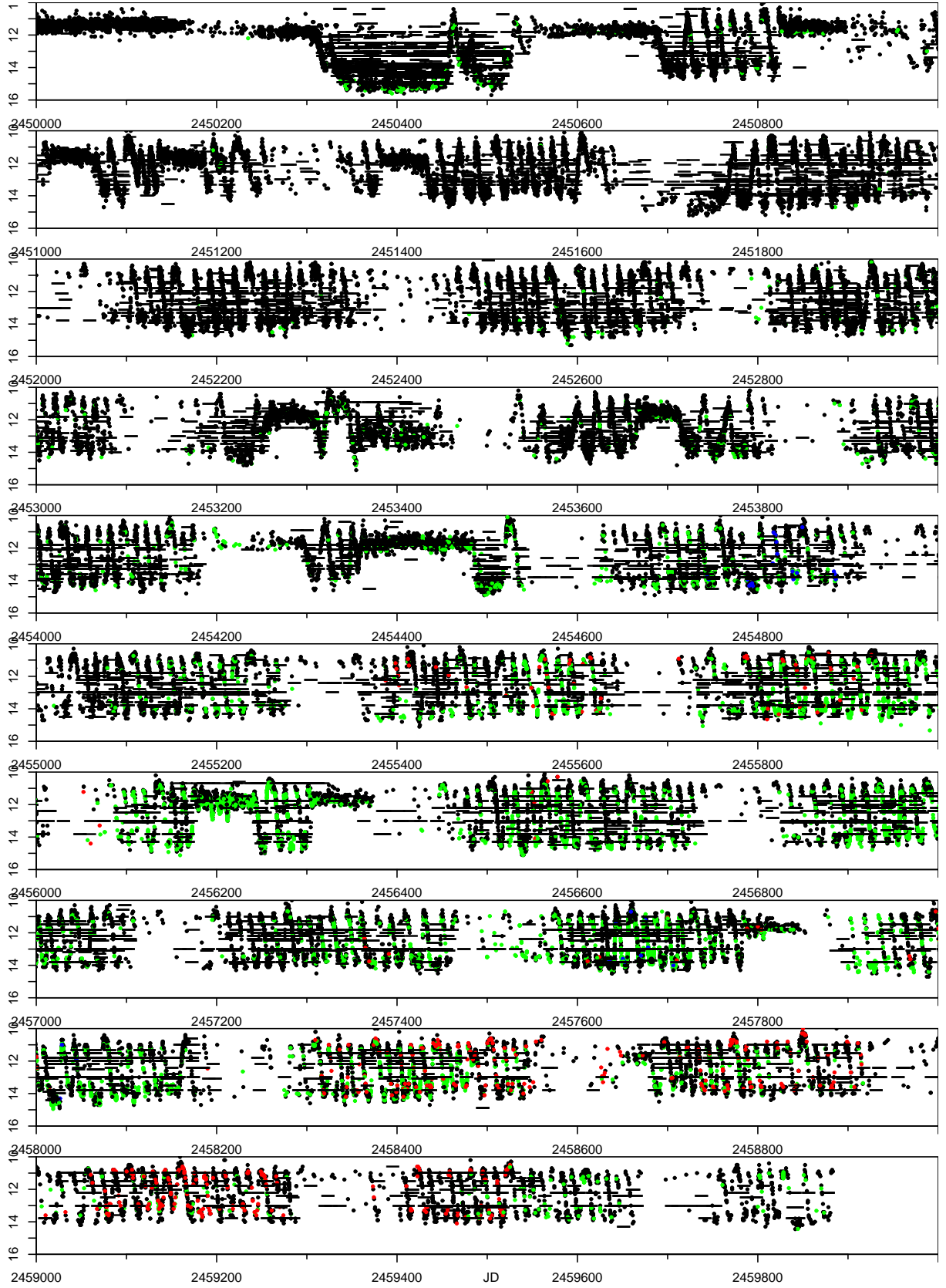


Fig. 3. RX And light curve of the entire span. The y-axis represents the magnitude. The color bands are as follows: the visual data (black circle), the V (green circle) or CV (blue circle) band on the CCD data, and the cG (red circle) band of digital camera photometry. The bar represents the upper limit when not observed. The bar represents the upper limit when not observed.

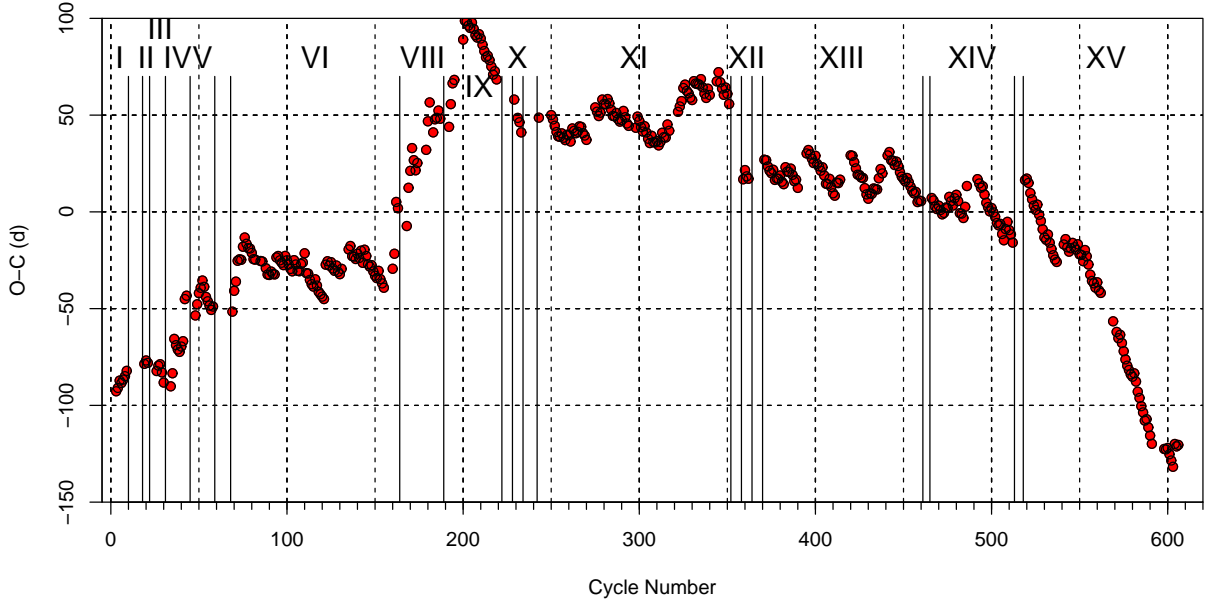


Fig. 4. The complete $O - C$ diagram of RX And. The x-axis represents the number of cycles, and the y-axis represents the $O - C$ value calculated with the ephemeris equation described in the paper. The Roman numbers I–XV represent the outburst phases (divided with solid lines).

Table 3. RX And Standstill List

	Period (JD - 2400000)	Duration (d)
SS I	50826 – 50965	139
SS II	51013 – 51068	55
SS III	51135 – 51186	51
SS IV	51384 – 51431	47
SS V	53265 – 53312	47
SS VI	53670 – 53710	40
SS VII	54203 – 54297	94
SS VIII	54366 – 54485	119
SS IX	56179 – 56245	66
SS X	56305 – 56375*	70
SS XI	57788 – 57860*	82
SS XII	58649 – 58681	32

* includes errors because of observational gap.

OP V and VI are distinguished by a declining state rather than a standstill.

the behavior called standstill. This oscillation had a period of approximately 80 ds and an amplitude of 2 magn. This behavior is also atypical of the general DN outburst. Although standstills with oscillations are known, these are not accompanied by a gradual decline.

In addition, gradual variations during 13 mag–15 mag were observed in the 2012 and 2013 seasons. This is also atypical of dwarf novae. After the typical standstill again appeared in the 2014 season, typical outbursts began to be observed, and the general DN outburst phase started. This uncharacteristic state continued during JD 2455400–2457150 (approximately 5 years). Therefore, the case of WW Cet cannot be regarded as the typical "standstill". Apart from this uncharacteristic state, no standstill is detected in the WW Cet data used. Therefore, the WW Cet light curve is divided into two phases: before and after the "standstill".

t_{rec} is significantly long for a Z Cam-type system. Bateson (1991) indicated that the mean t_{rec} of the WW Cet outburst is 30.70 d. However, t_{rec} is not identical (ranges from 18 to 44 d).

The period is determined to be 38.4(3) d by performing linear regression on the outburst dates. With this period, the ephemeris equation is as follows:

$$JD_{\text{os}} = 2450603 + 38.4(3) \times E$$

The complete $O - C$ diagram of the WW Cet outburst is shown in Figure 6. This diagram clearly shows the variation in t_{rec} because of the atypical "standstill". The mean t_{rec} of outbursts was 48 d before the "standstill". It varied to 31 d after the "standstill". This is similar to the value in Bateson (1991).

3.4. HL CMa

HL CMa was identified as an Einstein X-ray source 1E 0643.0-1648 (Fuhrmann 1980). This object was identified

3.3. WW Cet

WW Cet is the most complex case of the six objects.

This object was observed as 2.1937 Ceti by Luyten (1962). Paczynski (1963) indicated that it is a member of the Z Cam type. However, Warner (1987) and Ringwald et al. (1996) indicated the unavailability of evidence to demonstrate that WW Cet shows a standstill. However, Simonsen & Stubbings (2011) reported the first observation of WW Cet in a standstill state. This object is a "true" Z Cam-type DN.

However, this "standstill" phenomenon is highly peculiar. The entire light curve is shown in Figure 5, including this "standstill". Although the variations of WW Cet in the 2010 season was similar to a typical standstill, this object declined gradually with oscillations in the 2011 season. This is unlike

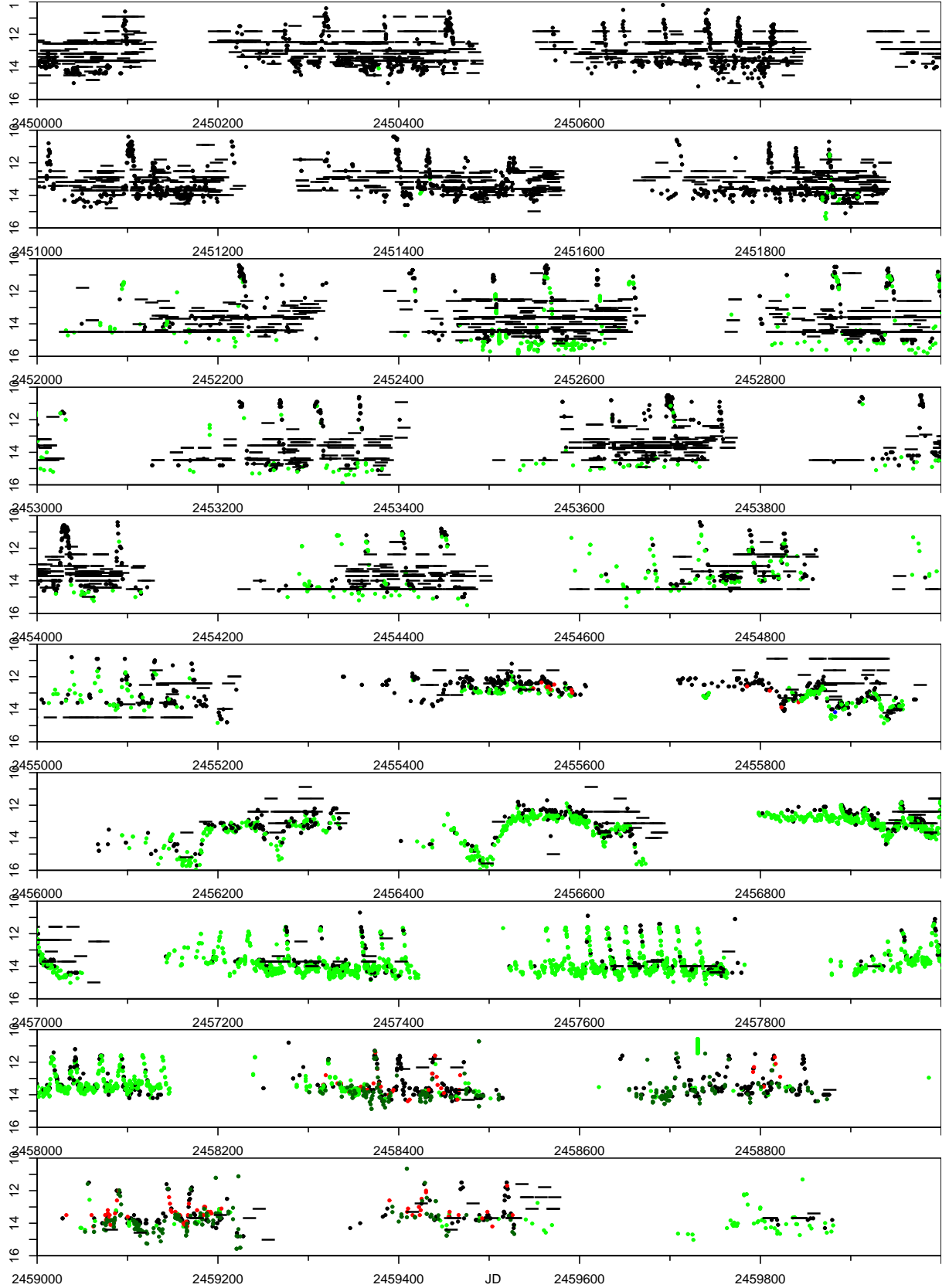


Fig. 5. The WW Cet light curve of the entire span. The y-axis represents the magnitude. The color bands are as follows: the visual data (black circle), the V (green circle) or CV (blue circle) band on the CCD data, the zg (dark green circle) band on the Zwicky data, the g (cyan circle) band on the ASASSN data, and the cG (red circle) band of digital camera photometry. The bar represents the upper limit when not observed. The bar represents the upper limit when not observed.

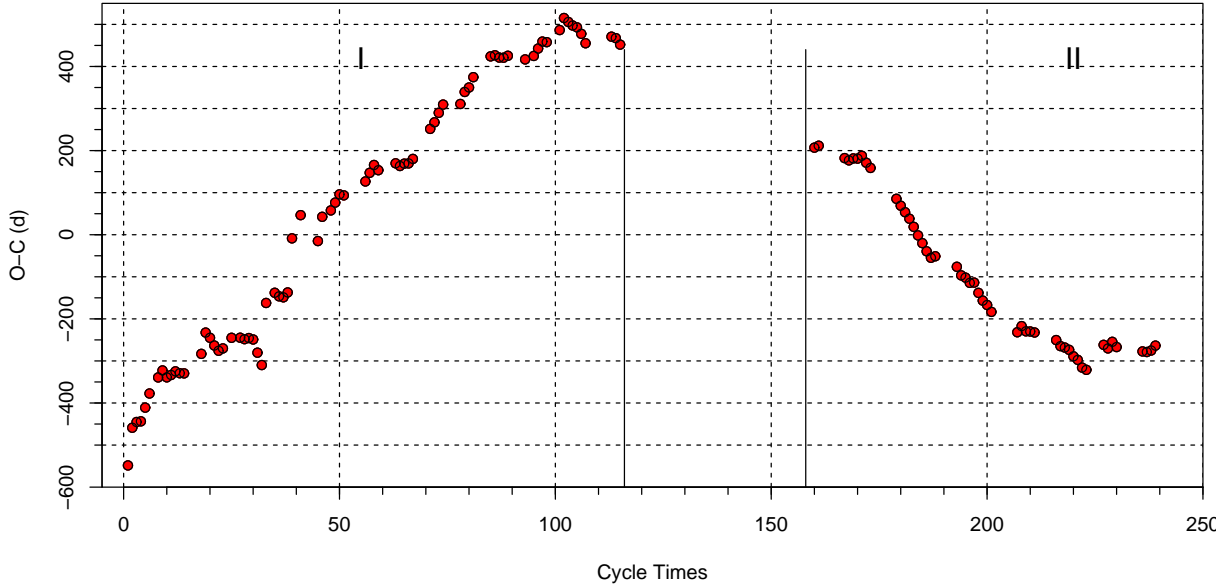


Fig. 6. The complete $O - C$ diagram of WW Cet. The x-axis represents the number of cycles, and the y-axis represents the $O - C$ value calculated with the ephemeris equation described in the paper. The Roman numbers I and II represent the outburst phases (divided with solid lines).

Table 4. WW Cet Standstill List

N	JD-2400000	Duration (d)
SS 1	55300* - 56900*	1600

* includes errors because of observational gap.

with an optical counterpart on a Harvard archive plate, which showed variability with a recurrence time of approximately 15 d. Therefore, this object was indicated as a dwarf nova (Chlebowski et al. 1981). The classification as Z Cam-type was recommended in the context of the orbital period and the interval of outbursts (Cannizzo et al. 1988). The existence of standstill was reported by AAVSO observations in 1982 (Mache & Raymond 1987). The definite long standstill was reported in 1999 (Watanabe et al. 2000). (Kato 2002) reported that HL CMa shows the third state neither, i.e. neither outburst or nor standstill (cyclic small variation).

HL CMa is recommended to be classified as a member of the new group of DNe: IW And-type. The IW And-type object is a new subgroup of DNe similar to the Z Cam-type. A characteristic of this type is that the standstill of this subgroup system terminates with the outburst (Kato 2019). Certain members of this subgroup are classified as Z Cam-type. Simonsen et al. (2014) reported certain objects displaying this behavior in Z Cam-type (including HL CMa).

The entire light curve is shown in Figure 7. According to the light curve, the light variations are divided into 11 outburst phases. These are terminated with standstill phases. The journal of standstill in HL CMa is summarized in Table 5. Because the quiescence of HL CMa is faint (15 mag), observations in the minimum are highly sparse. Thus, it is challenging to discuss the variations in luminosity in quiescence as identified in Z Cam and RX And.

The mean t_{rec} is estimated as 16.97(2) d by linear regression.

With this value, the ephemeris equation is as follows:

$$JD_{\text{os}} = 2549958 + 16.97(2)$$

OP II–III are peculiar phases. These correspond to the period reported by Kato (2002). Although a short (~ 60 d) standstill divides this stage into two phases, it is unclear whether this standstill (SS II) is real or not because of the sparsity of observations of the conjunction with the sun and small oscillation. This may be an oscillation phase with a low amplitude.

The standstill between OP VI and VII (SS VI) includes two standstills. However, only one outburst occurs between these two standstills. Therefore, this is not regarded as an outburst phase because an analysis using the $O - C$ diagram cannot be performed. This behavior wherein a few outbursts appear during standstill is generally detected in the light curve of IW And-type dwarf novae (Kato 2019). Although the light curve is unclear because of the seasonal gap, the transition of OP VII–VIII (SS VII) appears to be a similar case. This behavior of the light curve reveals that HL CMa shows the characteristics of IW And-type.

The $O - C$ diagram implies that HL CMa also has plural intervals of outbursts: 14–15 d and 19–20 d. These correspond to the downward-sloping and upward-sloping parts, respectively, in the $O - C$ diagram. Simonsen et al. (2014) indicated that this object also shows IW And-type behavior. The $O - C$ diagram implies that t_{rec} varies around $E > 350$. However, this is only an appearance.

3.5. AH Her

Similar to HL CMa, AH Her is reported to display the characteristic wherein the termination of standstill accompanies an outburst Simonsen et al. 2014. These two systems are classified as IW And-type (UGIW) in the VSX database.

This object was reported as a newly identified variable star in 1923 (Blažko 1923). Jacchia (1937) indicated the relation-

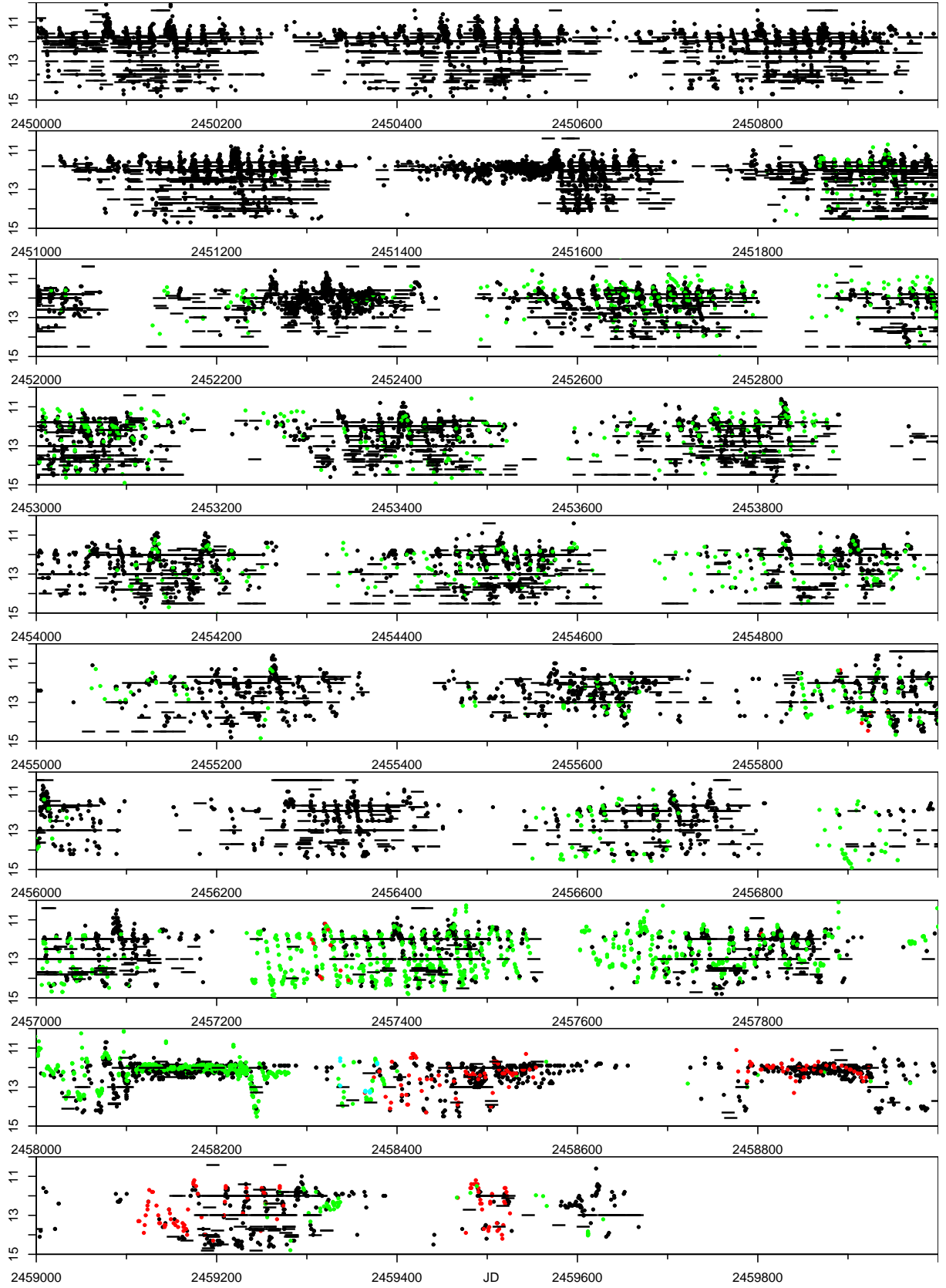


Fig. 7. The HL CMA light curve of the entire span. The y-axis represents the magnitude. The color bands are as follows: the visual data (black circle), the V (green circle) or CV (blue circle) band on the CCD data, the zg (dark green circle) band on the Zwicky data, the g (cyan circle) band on the ASASSN data, and the cG (red circle) band of digital camera photometry. The bar represents the upper limit when not observed.

Table 5. HL CMa Standstill List

	Period (JD–2400000)	Duration (d)	Remarks
SS I	51412–51570	158	TO
SS II	52230*–52250*	20	uncertain
SS III	52345–52415	70	TO
SS IV	53264–53310	46	
SS V	55668–55690	22	
SS VI	58110–58332*	222	O 58246
SS VII	58475–58565*	90	O 58506
SS VIII	58797–58925	128	
SS IX	59310–59352	42	TO
SS X	59557–59603	46	

*:large errors because of observational gap.

TO: outburst as the termination of standstill

O: outburst during standstill and its date

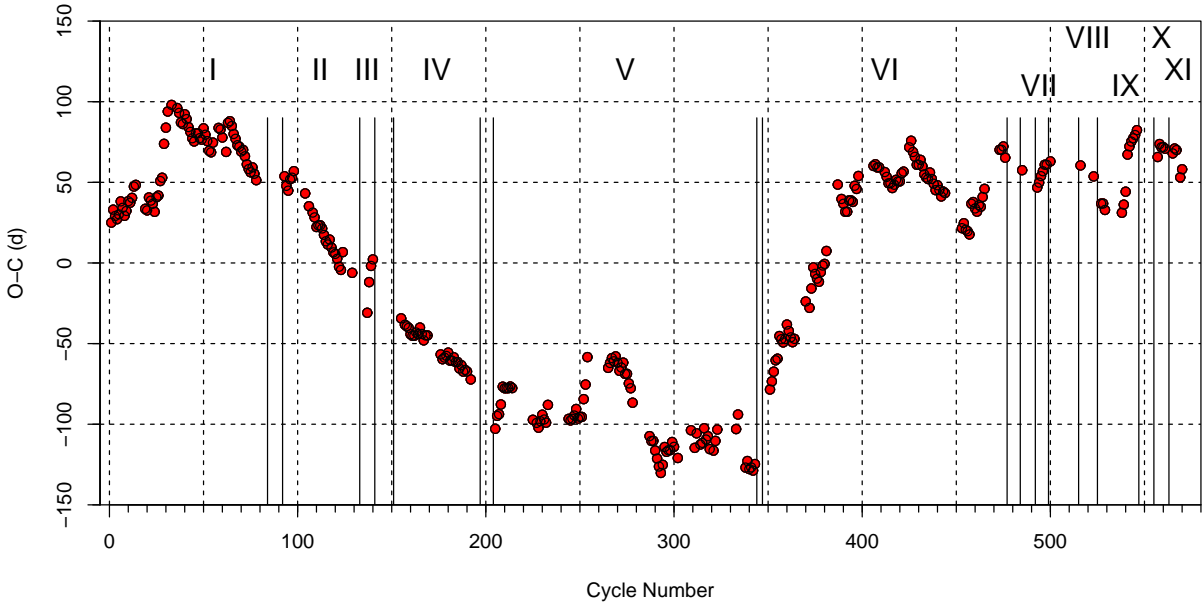


Fig. 8. The complete $O - C$ diagram of HL CMa. The x-axis represents the number of cycles, and the y-axis represents the $O - C$ value calculated with the ephemeris equation described in the paper. The Roman numbers I–XI represent the outburst phases (divided with solid lines).

ship with Z Cam. Jacchia (1937) reported a period of 19.5 d. Szkody & Mattei (1984) estimated the interval of outbursts as 18 d (scattering 7–27 d).

The mean t_{rec} is determined as 17.57(2) d by linear regression. With this value, the ephemeris equation is as follows:

$$JD_{\text{OS}} = 2450003 + 17.57 \times E$$

The $O - C$ diagram based on this ephemeris is shown in Figure 10.

The entire light curve is shown in figure 7. According to the light curve, the light variation is divided into 15 outburst phases (OP I–XV) and standstill phases between these. The journal of standstill in AH Her is summarized in Table 6.

Similar to HL CMa, the case wherein outbursts occur transiently during a standstill is observed. The standstill between OP II and III includes one or two outbursts. The standstill between IV and V displays a similar behavior. The standstill be-

tween OP X and XI show two such transitions. These behaviors show that AH Her is IW And-type.

The three characteristics indicated in the Z Cam section are also identified in AH Her. In particular, a decrease in the outburst duration is observed in many cases of OP. The increase in minimum magnitude is observable in this object. This may be expressed as oscillations.

In AH Her, OP VII is a peculiar phase. In this phase, the minimum magnitude is significantly high, frequently attaining 12.5 mag. This is almost as high as that in the standstill. The profile of outbursts in this OP is atypical for the Z Cam type. The increase and decrease are highly steep. Finally, the outburst frequency reduces, and the standstill starts.

The early phase in OP X shows the converse behavior. The luminosity attains approximately 12.5 mag even with the maximum outburst at that time. The luminosity in the quiescence

Table 6. AH Her Standstill List

	Period (JD-2400000)	Duration (d)	Remarks
SS I	50722–50744	22	
SS II	50830*–51024	194	O 50958
SS III	52390–52433	43	
SS IV	52480–54822	342	O 52778
SS V	53425–53472	27	TO
SS VI	54391–54485	94	TO
SS VII	54910–55417	507	
SS VIII	55860–56264	404	O 56018, 56107
SS IX	57042–57169	127	TO suspected
SS X	57377–57608	43	O 57425
SS XI	58016–58029	13	TO
SS XII	58100–58138	38	TO
SS XIII	59784–59816	32	TO

* includes errors because of observational gap.

TO: outburst as the termination of standstill

O: outburst during standstill and its date

is similar to the general OP (14 mag).

Notably, the quiescent magnitude of AH Her is generally high (~ 12.5 mag) when the next standstill is not being approached.

3.6. SY Cnc

SY Cnc is classified as RW Aur-type (a subgroup of the pre-main sequence star) in the first edition of GCVS. However, Herbig (1950) revealed that the spectrum of SY Cnc is similar to those of DNe such as SS Cyg and Z Cam.

Although SY Cnc is classified as Z Cam-type DN, the observational report of standstill is highly sparse. Only two short standstills are detected in the used data of approximately 25 years. In addition, one of the standstills is suspect because it may be a long outburst. Szkody & Mattei (1984) estimated the mean t_{rec} as 27 d, and t_{rec} scatters during 22–35 d.

The entire light curve is shown in Figure 11. As described above, this object shows a standstill infrequently. Meanwhile, the seasonal gap is pronounced because this object is close to the zodiac. t_{rec} is determined as 26.330(17) d by linear regression. This value is close to that presented in Szkody & Mattei (1984).

The ephemeris equation is obtained as follows with this t_{rec} :
 $JD_{\text{os}} = 2449887 + 26.330 \times E$

The $O - C$ diagram obtained is shown in Figure 12. It indicates that SY Cnc displays variations in t_{rec} regardless of the sparsity of standstill. There are two types of intervals. The shorter one is 23.5 d, and the longer one is 28 d. However, a gradual variation in t_{rec} is observed in this object. The intermediate period is also observed. It is nearly equal to the "average" length. It is noteworthy that this variation is not related to the standstill.

Table 7. SY Cnc Standstill List

	Period (JD-2400000)	Duration (d)	Remarks
SS I	56259 - 56283	25	
SS II	57110 - 57137	27	uncertain

4. Discussion

The standstill frequency and durations differ among the six objects. However, their $O - C$ diagrams indicate that all the systems show a secular variation in outburst frequency.

It is notable that t_{rec} reduces as the next standstill is approached in almost all the cases among four objects (Z Cam, RX And, AH Her, and HL CMa) except for the cases in the highly peculiar states. Similarly, the enhanced luminosity in the quiescence state is also interpreted as the enhancement of the disk luminosity.

These two characteristics are explained by the variation in mass transfer rate. Meanwhile, the long outbursts extinct before the occurrence of standstill causes a decrease in the mass accretion from the disk. This is considered to result in an increase in the column density of the disk and the start of the standstill.

It is noteworthy that the luminosity in quiescence is occasionally not enhanced. Meanwhile, the disappearance of the long outburst is observed in almost all cases. This disappearance can be interpreted as an enhanced mass transfer rate.

Another problem is the variation trend of t_{rec} . Certain systems (RX And and AH Her) show a cyclic variation in the quiescent luminosity during the long-term outburst phase. Because t_{rec} shortens during bright quiescence, this can be explained by the increased column density of the disk. However, the $O - C$ diagrams indicate an abrupt variation in t_{rec} although the cyclic variation in quiescent luminosity is gradual.

SY Cnc shows the variation in t_{rec} during an outburst phase, particularly OP I. The abrupt variation in period occurs for E ~ 120 (JD *sim* 2455300) and 190 (JD ~ 2454800). Both abrupt shortening of the interval. The light curves do not show peculiarity in these timings.

In addition, the t_{rec} in a system tends to display two values. This is difficult to explain. SY Cnc has two typical intervals: 23.5 d and 28 d. HL CMa has two types of intervals: 14–15 d and 19–20 d. The intervals for RX And are 13 d and 17 d, and those for Z Cam are 22d and 33d. AH Her shows more than two typical outburst intervals.

Finally, WW Cet is the most puzzling object in this research. The irregular state observed during the early 10s may have been a true standstill. However, this may be related to the variation in mass transfer rate at any rate. t_{rec} varied after this irregular state.

4.1. Acknowledgement

I acknowledge with gratitude the variable star observations obtained from the AAVSO International Database and VSNET International Database contributed by observers worldwide and used in this research. I also acknowledge with gratitude the data obtained by ASAS-3, ASASSN, and The

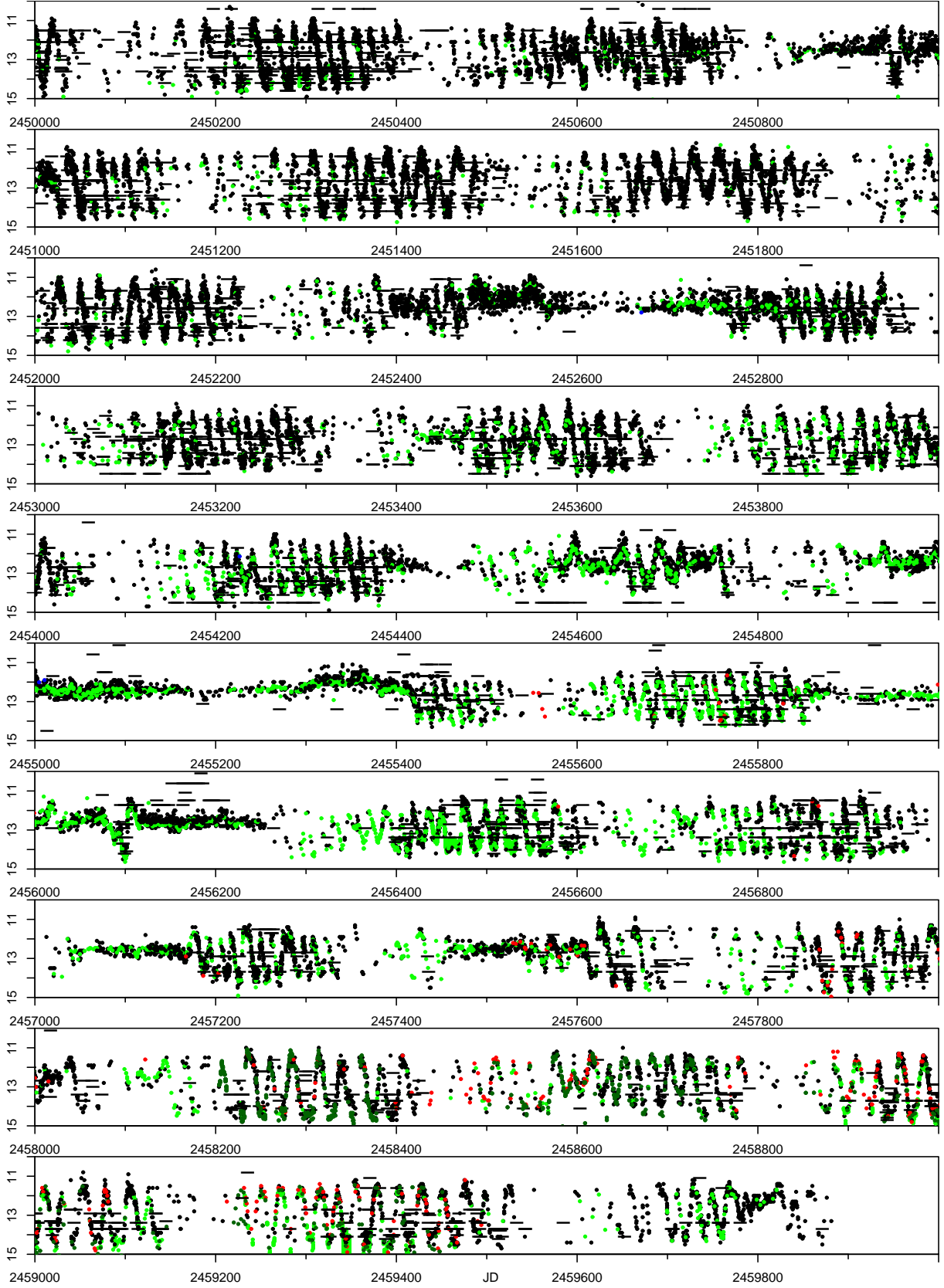


Fig. 9. The AH Her light curve of the entire span. The y-axis represents the magnitude. The color bands are as follows: the visual data (black circle), the V (green circle) or CV (blue circle) band on the CCD data, the zg (dark green circle) band on the Zwicky data, the g (cyan circle) band on the ASASSN data, and the cG (red circle) band of digital camera photometry. The bar represents the upper limit when not observed.

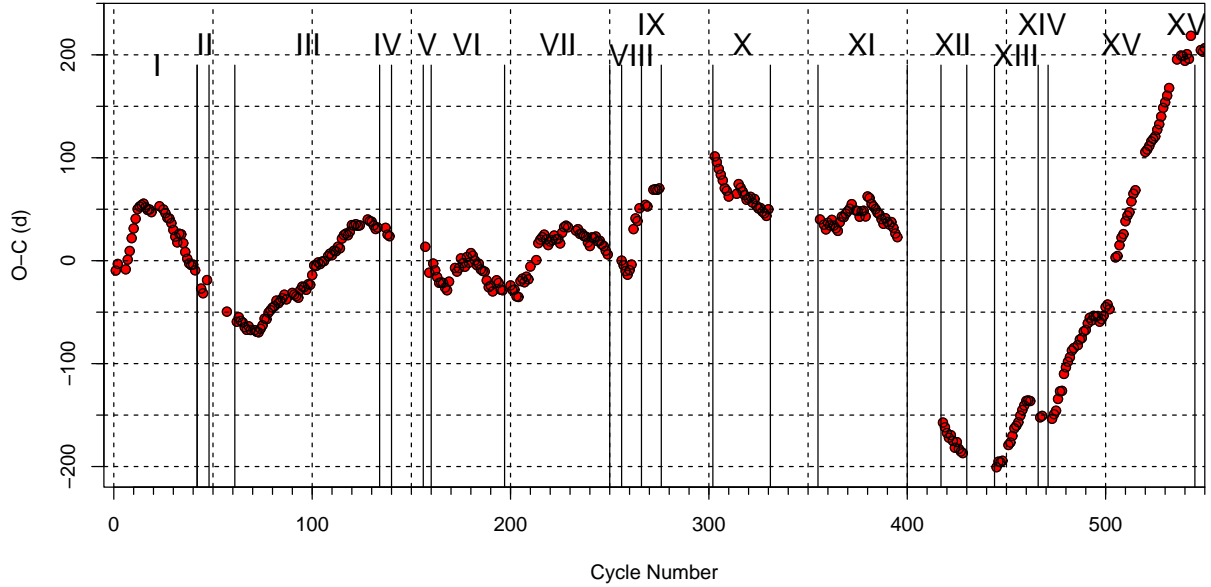


Fig. 10. The complete $O - C$ diagram of AH Her. The x-axis represents the number of cycles, and the y-axis represents the $O - C$ value calculated with the ephemeris equation described in the paper. The Roman numbers I–XV represent the outburst phases (divided with solid lines).

Zwicky Transient Facility. I also would like to thank Editage (www.editage.com) for English language editing.

References

- Bath, G. T. 1973, *Nature. Physical Science*, 246, 84
- Bellm, E. C. et al. 2019, *Publications of the Astronomical Society of the Pacific*, 131, 018002
- Bateson, F. M. and McIntosh, R. 1991, *Royal Astronomical Society of New Zealand Publications of Variable Star Section*, 16, 70
- Blažko, S. 1923, *Astron. Nachr.*, 219, 372
- Cannizzo, J. K., Shafter, A. W., and Wheeler, J. C. 1988, *Astrophysical Journal*, 333, 227
- Chlebowski, T., Halpern, J. P., and Steiner, J. E. 1981, *Astrophysical Journal*, 247, L35
- de Roy, F. 1932, *Gazette Astronomique*, 19, 1
- Fuhrmann, B. 1980, *Information Bulletin on Variable Stars*, 1883
- Jacchia, L. 1937, *Astron. Nachr.*, 261, 212
- Herbig, G. H. 1950, *Publications of the Astronomical Society of the Pacific*, 62, 211
- Hellier, C. 2001, *Cataclysmic Variable Stars: How and why they vary* (Berlin: Springer-Verlag)
- Jayasinghe, T. et al. 2021, *MNRAS*, 503, 200
- Kafka, S. 2021, *Observations from the AAVSO International Database*, <https://www.aavso.org>
- Kato, T. 2001, *Information Bulletin on Variable Stars*, 5093
- Kato, T. 2002, *Information Bulletin on Variable Stars*, 5243
- Kato, T., Nogami, D., and Masuda, S. 2002, *Publications of the Astronomical Society of Japan*, 54, 575
- Kato, T., Uemura, M., Ishioka, R., Nogami, D., Kunjaya, C., Baba, H., and Yamaoka, H. 2004, *Publications of the Astronomical Society of Japan*, 56, S1
- Kato, T. 2019, *Publications of the Astronomical Society of Japan*, 71, 20
- Kato, T. 2021, *VSOLJ Bulletin*, 87, 1
- Luyten, W. J. 1962, *Harvard Observatory Announcement Card*, 1574
- Mauche, C. W. and Raymond, J. C. 1987, *Astrophysics & Space Science*, 130, 269
- Masci, F. J. et al. 2019, *Publications of the Astronomical Society of the Pacific*, 131, 018003
- Meyer, F. and Meyer-Hofmeister, E. 1983, 121, 29
- Nijland, A. A. 1930, *Bulletin of the Astronomical Institute of the Netherlands*, 5, 243
- Ohshima, T. et al. 2014, *Publications of the Astronomical Society of Japan*, 66, 63
- Oppenheimer, B. D., Kenyon, S. J., and Mattei, J. A. 1998, *Astronomical Journal*, 115, 1175
- Osaki, Y. 1974, *Publications of the Astronomical Society of Japan*, 26, 429
- Osaki, Y. 1996, *Publications of the Astronomical Society of the Pacific*, 108, 39
- Osaki, Y. and Kato, T. 2013, *Publications of the Astronomical Society of Japan*, 65, 50
- Osaki, Y. and Kato, T. 2013, *Publications of the Astronomical Society of Japan*, 64, 95
- Paczynski, B. 1963, *Publications of the Astronomical Society of the Pacific*, 75, 278
- Pojmański, G. 2002, *Acta Astronomica*, 52, 397
- Ringwald, F. A., Thorstensen, J. R., Honeycutt, R. K., and Smith, R. C. 1996, *Astronomical Journal*, 111, 2077
- Ritter, H. and Kolb, U. 2003, *Astronomy & Astrophysics*, 404, 301
- Ross, J. and Latter, H. N. 2017, *MNRAS*, 470, 34
- Shafter, A. W., Cannizzo, J. K., and Waagen, E. O. 2005, *Publications of the Astronomical Society of the Pacific*, 117, 931
- Shappee, B. J. et al. 2014, *Astrophysical Journal*, 788, 48
- Simonsen, M. and Stubbings, R. 2011, *J. American Assoc. Variable Star Obs.*, 39, 73
- Simonsen, M. et al. 2014, *JAASO*, 42, 177
- Szkody, P. and Mattei, J. A. 1984, *Publications of the Astronomical Society of the Pacific*, 96, 988
- Warner, B. 1987, *Monthly Notices of the Royal Astronomical Society*, 227, 23
- Warner, B. 1995, *Cataclysmic Variable Stars* (Cambridge: Cambridge University Press)

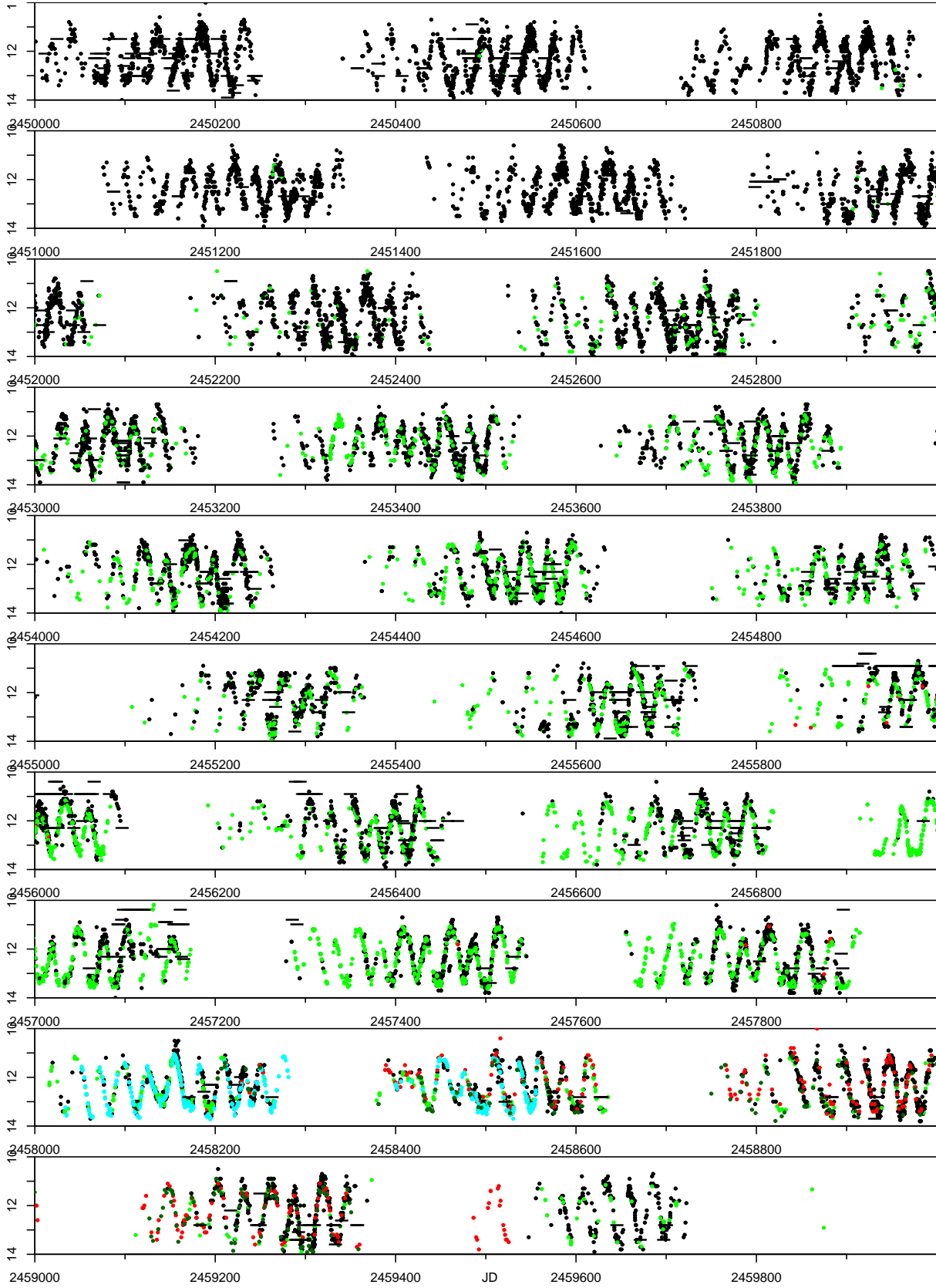


Fig. 11. The SY Cnc light curve of the entire span. The y-axis represents the magnitude. The color bands are as follows: the visual data (black circle), the V (green circle) or CV (blue circle) band on the CCD data, the zg (dark green circle) band on the Zwicky data, the g (cyan circle) band on the ASASSN data, and the cG (red circle) band of digital camera photometry. The bar represents the upper limit when not observed.

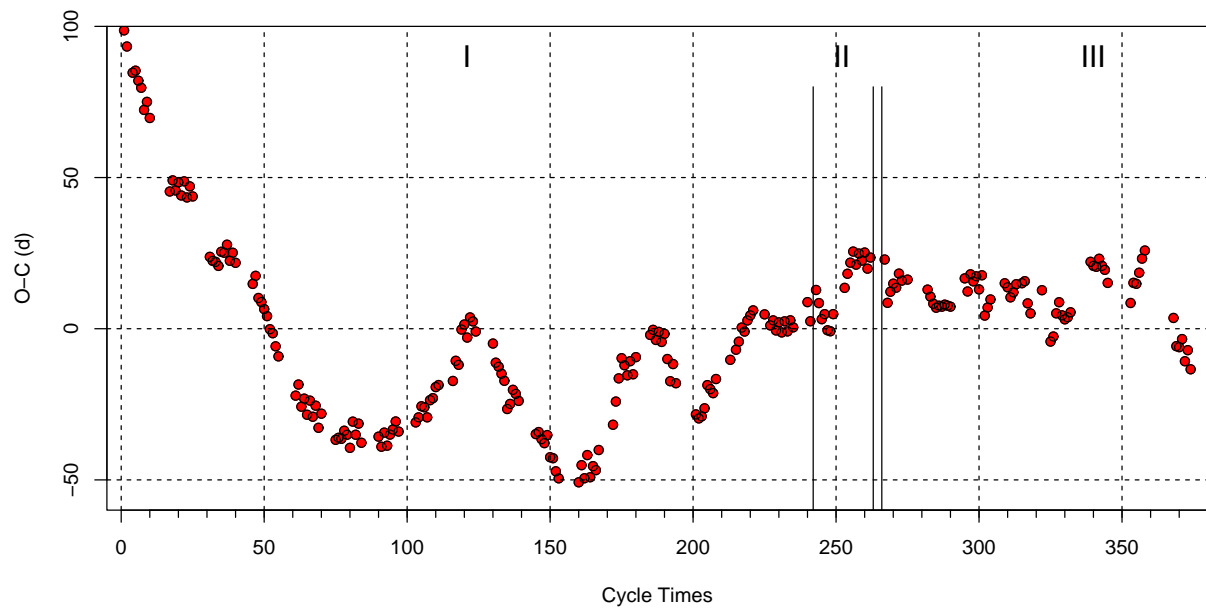


Fig. 12. The complete $O - C$ diagram of SY Cnc. The x-axis represents the number of cycles, and the y-axis represents the $O - C$ value calculated with the ephemeris equation described in the paper. The Roman numbers I–III represent the outburst phases (divided with solid lines).

Watanabe, T. and Stubbings, R., and Maehara, H. 2000, VSOLJ
Bulletin, 35-36, 7